Thermal and Starvation Effects on Lubricated Elliptical Contacts at High Rolling/Sliding Speeds

Vinod Kumar, Surjit Angra

Abstract—The objective of this theoretical study is to develop simple design formulas for the prediction of minimum film thickness and maximum mean film temperature rise in lightly loaded high-speed rolling/sliding lubricated elliptical contacts incorporating starvation effect. Herein, the reported numerical analysis focuses on thermoelastohydrodynamically lubricated rolling/sliding elliptical contacts, considering the Newtonian rheology of lubricant for wide range of operating parameters, namely load characterized by Hertzian pressure (PH = 0.01 GPa to 0.10 GPa), rolling speed (>10 m/s), slip parameter (S varies up to 1.0), and ellipticity ratio (k = 1 to 5). Starvation is simulated by systematically reducing the inlet supply. This analysis reveals that influences of load, rolling speed, and level of starvation are significant on the minimum film thickness. However, the maximum mean film temperature rise is strongly influenced by slip in addition to load, rolling speed, and level of starvation. In the presence of starvation, reduction in minimum film thickness and increase in maximum mean film temperature are observed. Based on the results of this study, empirical relations are developed for the prediction of dimensionless minimum film thickness and dimensionless maximum mean film temperature rise at the contacts in terms of various operating parameters.

Keywords—Starvation, lubrication, elliptical contact, traction, minimum film thickness.

I. INTRODUCTION

SINCE last 40 years, research has been devoted to a better understanding of a lubrication regime which occurs in non-conformal contacts of the machine elements such as gears, rolling bearings, cams etc. In such types of concentrated contacts, pressures become very high and the contacting surfaces deform elastically. In this condition, the viscosity of the lubricant may rise significantly which assists the formation of an effective fluid film in the contact. Such lubricated contacts are called elastohydrodynamically lubricated (EHL) contacts. In EHL contacts, the estimation of minimum film thickness, maximum mean film temperature and traction are important requirements from the design point of view of mechanical components. The birth of elastohydrodynamic (EHD) lubrication took place in the 1940s. A very important step in the investigation of point contacts lubrication was recorded in 1961 through the experimental work of Archard and Kirk [1]. Before the publication of this paper, it had been considered that only boundary lubrication could occur under

such extreme conditions. Archard and Kirk's experiments with crossed cylinders showed that the values of film thickness at a point contact with a circular Hertzian region differed less than might have been expected from those at a line contact. A comparison of the values of film thickness for a line contact [2] with those for a point contact [1] under similar conditions shows that the two values differ by roughly a factor of 2. Due to lack of computing power and mathematical complexity, the solution of two-dimensional EHD (i.e. point contact) problem was delayed till the 1970s. Now, that the line contact problem was considered to be solved, but there were needs to develop solutions for specific components such as ball bearings which exhibit elliptical contacts. The solution attempts of lubricated elliptical contacts started with Newtonian fluids for isothermal conditions. The earliest theory of the lubrication of spheres came through Kapitza [3]. In the mid-1960s, Cameron and Gohar [4] and Archard and Cowking [5] presented interesting approximate solutions to the problem of lubricated elliptical contacts. Cheng [6] also undertook a similar study of the inlet region alone on the basis of the solution of the Reynolds equations by finite difference methods (FDM). Full direct numerical solutions in which the Reynolds equation and elasticity equations are simultaneously satisfied for point contacts, emerged in the mid-1970s. Ranger et al. [7] used a straight forward iterative method and developed results for circular contacts for various values of the load, speed and pressure viscosity coefficient. Dowson and Hamrock [8] and Biswas and Snidle [9] have presented numerical evaluation of surface deformations in point contact. Hamrock and Dowson [10]-[12] have carried out a comprehensive range of numerical solutions for fully flooded and starved point contacts in which the influence of ellipticity ratio is considered. References [7], [12], [13] have given empirical relations for prediction of film thickness under isothermal conditions at low loads and low speeds. The use of such film thickness relations involves a significant degree of extrapolation at heavy loads, which results in overestimation of film thickness. Numerical stability and computational cost were the concern of early computations in the EHL field. In 1992, Venner and Napel [14], [15] presented a fast numerical solver for the EHL circular contact problems. Full numerical analyses of the EHD lubrication problem of a circular point contact have been reported by [16], [17].

Thermal effects have an important impact on the performance of highly loaded lubricated contacts such as those found in high-speed rolling bearings, cams and tappets, gears, and traction drives. Under severe operating conditions shearing of the lubricant brings heat dissipation which

Vinod Kumar is with the National Institute of Technology, Kurukshetra - 136118, Haryana, India (phone: +919729030269; fax: +911744233557; e-mail: mit_vkum@hotmail.com).

Surjit Angra is with the National Institute of Technology, Kurukshetra - 136118, Haryana, India (phone: +919416993047; fax: +911744233557; e-mail: angrasurjit@yahoo.com)

influences both the film thickness and the traction characteristics at the contact. Bruggemann and Kollmann [18] were the first to include thermal effects in the study of elliptical contacts. Kim and Sadeghi [19], [20] presented a full thermal EHL point contact analysis in which they obtained solutions for pure rolling and low slip conditions. Their calculations revealed a significant inlet shear heating even under pure rolling conditions. To avoid the costly discretization across the film required by the energy equation, a parabolic temperature profile across the film thickness has been often adopted by an investigator which allows the three-dimensional problem to be transformed to a two-dimensional analysis. Such an assumption was applied by [21], [22] and recently [23] in line contact problems. Jiang et al. [24], Lee et al. [25] and Ehret et al. [26] adopted the same type of simplification to solve elliptical and point contact problems.

Engineering surfaces although appear smooth to the naked eye are quite rough on microscopic level. The height of surface roughness significantly modifies pressure, temperature, and internal stresses within the rolling/sliding contacts. Thus, increasingly effort has been devoted to the study of EHL contacts with surface roughness. Gang and Sadeghi [27], Zhu and Hu [28], and Yang et al. [29] have tried to study thermal effects in point/elliptic contacts by incorporating roughness effects under certain assumptions and limitations.

Literature survey reveals that for the combinations of the light loads (maximum Hertzian pressure in the range 0.01 GPa - 0.1 GPa), high rolling speeds (10 to 30 m/s), high slips (25 to 50%), ellipticity ratio (1 to 5), and roughness (0 to 0.2 μm) values existing in the ball bearings of aircrafts, no thermal EHL analysis have been carried out for fully flooded conditions for the characteristic study of film thickness, mean film temperature and traction. Therefore, an attempt has been made to carry out an efficient thermal EHL analysis of elliptic contacts for the above range of operating parameters and to develop empirical relations for the prediction of minimum film thickness, maximum non dimensional mean film temperature rise, and traction coefficient.
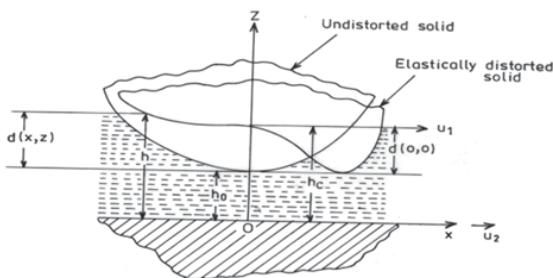
II. GOVERNING EQUATIONS

Fig. 1 Coordinate system

EHD lubrication of concentrated contacts involves the elastic deformation of non-conformal mating surfaces due to very high pressure generated at the contact within the thin lubricating film. The performance parameters of EHL

concentrated contacts can be computed by coupled solution of governing equations (viz. Reynolds equation, energy equation, film shape (including surface deformations), and rheological relations of lubricant) by incorporating appropriate boundary conditions. The coordination system adopted is shown in Fig. 1.

A. Film Thickness Equation

In EHD, the mating surfaces deform elastically. An expression for lubricant film thickness in a 3-D EHD contact is written as:

$$h(x,y,z) = h_0 + \frac{x^2}{2R_x} + \frac{y^2}{2R_y} + d(x,y,z) - d(0,0,0) \tag{1}$$

The elastic deformation $d(x, y, z)$ in (1) is evaluated:

$$d(x,y,z) = \frac{2}{\pi E'} \int_{y'=-\infty}^{y'=\infty} \int_{x'=-\infty}^{x'=\infty} \frac{p(x,y)}{[(x-x')^2 + (y-y')^2]^{1/2}} dx' dy' \tag{2}$$

There are two main problems associated with the numerical evaluation of this integral. The first problem arises due to singularity i.e., when $(x, y) = (x', y')$. The second problem comes due to involved computations. If the elastic deformations at all the grids N xN of domain are being computed, then the time in numerical integration of (2) is proportional to N^4. To cut short the computational time, it is essential to use relatively coarse finite difference grids in domain. The usual method of dealing with the singularity in (2) is to replace the integration with an analytic expression in the region of singularity. It is assumed that the pressure in the region of the singularity is constant all over the nine grid points (the point of interest and the eight grid points around it). Fig. 1 explains the nine grid point concepts. In the light of Fig. 1, (2) is analytically integrated and written as:

$$d(x,y,z) = p(x,y) \times D \tag{3}$$

where D is the elastic influence coefficient and given as:

$$D = \frac{2}{\pi E'} \begin{bmatrix} (x+m_1)\ln\frac{(y+n_1)+\{(x+m_1)^2+(y+n_1)^2\}^{1/2}}{(y-n_2)+\{(x+m_1)^2+(y-n_2)^2\}^{1/2}} \\ +(x-m_2)\ln\frac{(y-n_2)+\{(x-m_2)^2+(y-n_2)^2\}^{1/2}}{(y+n_1)+\{(x-m_2)^2+(y+n_1)^2\}^{1/2}} \\ +(y+n_1)\ln\frac{(x+m_1)+\{(x+m_1)^2+(y+n_1)^2\}^{1/2}}{(x-m_2)+\{(x-m_2)^2+(y+n_1)^2\}^{1/2}} \\ +(y-n_2)\ln\frac{(x-m_2)+\{(x-m_2)^2+(y-n_2)^2\}^{1/2}}{(x+m_1)+\{(x+m_1)^2+(y-n_2)^2\}^{1/2}} \end{bmatrix} \tag{4}$$
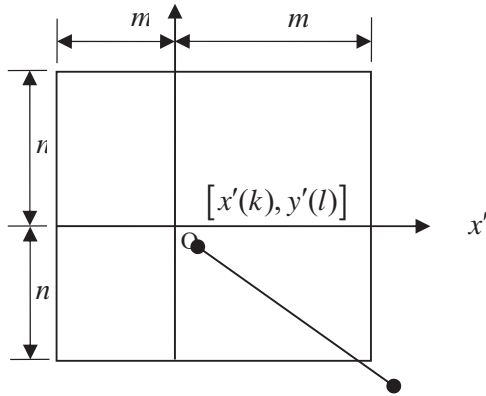
Fig. 2 Pressure element shape and local coordinates

The variables m_1, m_2, n_1 and n_2 in (4) are shown in Fig. 2. Thus, the elastic deformation caused by the pressures acting over the lubrication region can be written as:

$$d(i,j) = \sum_k \sum_l D(i,j,k,l) \times p(k,l) \qquad (5)$$

where, $D(i, j, k, l)$ refers to the elastic influence coefficient at grid point (i, j) caused by unit pressure acting over the rectangular element at grid (k, l).

B. Reynolds Equation

The Reynolds equation for steadily flow in 3-D form is as

$$\frac{\partial}{\partial x}\left(\frac{\rho h^3}{\eta}\frac{\partial p}{\partial x}\right) + \frac{\partial}{\partial y}\left(\frac{\rho h^3}{\eta}\frac{\partial p}{\partial y}\right) = 12u\frac{\partial}{\partial x}(\rho h) \qquad (6)$$

C. Energy Equation

The prediction of the temperature rise in the EHL contact can be done accurately by the energy conservation law at a point in the lubricant film. Energy equation in its steady-state form, with no external sources of film heating can be expressed in the Cartesian coordinates as:

$$\rho\, C_p\left(u\frac{\partial T}{\partial x} + v\frac{\partial T}{\partial y}\right) = \frac{\partial}{\partial z}\left(k_f\frac{\partial T}{\partial z}\right) + \eta\left[\left(\frac{\partial u}{\partial z}\right)^2 + \left(\frac{\partial v}{\partial z}\right)^2\right] \qquad (7)$$

where

$$u = -z\frac{h-z}{2\eta}\frac{\partial p}{\partial x} + u_1\frac{h-z}{h} + u_2\frac{z}{h} \qquad (8)$$

$$v = -z\frac{h-z}{2\eta}\frac{\partial p}{\partial y} \qquad (9)$$

The convective term $w\frac{\partial T}{\partial z}$ in the energy equation is neglected since the velocity, w, in z-direction is zero.

Across the lubricating film thickness, a parabolic temperature profile is adopted for simplification of the computation of energy equation. This assumption reduces 3-D energy equation into a 2-D equation.

The equation for parabolic temperature profile across the film is as:

$$T(x,y,z) = (3T_1 + 3T_2 - 6T_m)\left(\frac{z}{h}\right)^2 + (6T_m - 4T_1 - 2T_2)\left(\frac{z}{h}\right) + T_1 \qquad (10)$$

where $T_1(x, y)$ and $T_2(x, y)$ are the temperatures of the bounding surfaces and $T_m(x, y)$ represents the mean temperature across the film. Substituting (8)-(10) into the energy equation (7) and integrating the equation across the z direction from '0' to 'h', the following simplified form of the energy equation is obtained:

$$6T_1 + 6T_2 - 12T_m - \frac{\rho C_p h^4}{120 k_f \eta}\frac{\partial p}{\partial x}\left(\frac{\partial T_1}{\partial x} + \frac{\partial T_2}{\partial x} - 12\frac{\partial T_m}{\partial x}\right)$$
$$-\frac{\rho C_p h^4}{120 k_f \eta}\frac{\partial p}{\partial y}\left(\frac{\partial T_1}{\partial y} + \frac{\partial T_2}{\partial y} - 12\frac{\partial T_m}{\partial y}\right) - \frac{\rho C_p u h^2}{k_f}\frac{\partial T_m}{\partial x} - \qquad (11)$$
$$\frac{\rho C_p u S h^4}{12 k_f}\left(\frac{\partial T_2}{\partial x} - \frac{\partial T_1}{\partial x}\right) + \frac{h^4}{12 k_f \eta}\left[\left(\frac{\partial p}{\partial x}\right)^2 + \left(\frac{\partial p}{\partial y}\right)^2\right] + \frac{\eta u^2 S^2}{k_f} = 0$$

The boundary conditions for the energy equation, for two moving surfaces, are given as:

$$T_1(x,y) = \left(\frac{1}{\pi \rho_1 c_1 u_1 k_1}\right)^{1/2}\int_{-\infty}^{x} k_f \left.\frac{\partial T(x,y)}{\partial z}\right|_{z=0}\frac{d\psi}{(x-\psi)^{1/2}} \qquad (12)$$

$$T_2(x,y) = \left(\frac{1}{\pi \rho_2 c_2 u_2 k_2}\right)^{1/2}\int_{-\infty}^{x} k_f \left.\frac{\partial T(x,y)}{\partial z}\right|_{z=h}\frac{d\psi}{(x-\psi)^{1/2}} \qquad (13)$$

D. Rheological Relations for Lubricant

The density model used in the present EHD lubrication is:

$$\rho = \rho_0\left(1 + \frac{0.6\times10^{-9} p}{1 + 1.7\times10^{-9} p}\right)\left[1 - \beta(T - T_0)\right] \qquad (14)$$

The Roelands' viscosity model is used in the present analysis

$$\eta = \eta_0 \exp\left\{\left(\ln(\eta_0) + 9.67\right)\left[-1 + \left(1 + 5.1\times10^{-9} p\right)^z\right] - \gamma(T - T_0)\right\} \qquad (15)$$

Lubricant and disks properties have been listed in Table I.

E. Traction Model

Traction allows the transmission of mechanical energy rather than its dissipation. In hydrodynamic lubrication the Newtonian traction model can be represented as:

$$F = \pm \iint_{\Omega} \tau_{0,h} \, dx \, dy \qquad (16)$$

where, F = Traction force; Ω = Domain of lubrication

$$\tau_{0,h} = \frac{\eta}{h} \Delta u + \frac{h}{2} \frac{\partial p}{\partial x} \quad \text{and} \quad \Delta u = u_1 - u_2$$

F. Surface Roughness Model

All engineering surfaces are rough. The profile of a rough surface is always random unless some regular features have been deliberately introduced. The influence of the surface roughness has been studied by many researchers. Random distribution of roughness asperities makes it less realistic to assume any deterministic models of surface roughness to model real engineering surfaces. Thus the present study incorporates the application of the stochastic model to quantify the distribution of roughness.

The stochastic theory assumes the film thickness h, comprises of two parts- (i) nominal or smooth part of the geometry $h_n(x, y, z)$, and (ii) the part due to surface roughness $h_s(x, y, \xi)$ as measured from the nominal level. The nominal film thickness component is a function of only space coordinates whereas the surface roughness part is also a function of a random variable ξ, in addition to the space coordinates. Assigning a particular value to ξ is to be interoperated as selecting a particular roughness arrangement.

By taking the expected value of the Reynolds equation (6) on both the sides, the Reynolds equation becomes:

$$\frac{\partial}{\partial x} E\left(\frac{\rho h^3}{\eta} \frac{\partial p}{\partial x} \right) + \frac{\partial}{\partial y} E\left(\frac{\rho h^3}{\eta} \frac{\partial p}{\partial y} \right) = 6(u_1 + u_2)\frac{\partial}{\partial x}(\rho E(h)) \qquad (17)$$

where the expectancy function, $E(x)$, is defined as

$$E(x) = \int_{-\infty}^{+\infty} x \, f(x) \, dx \qquad (18)$$

In (18) f (x) is the probability density distribution for the stochastic variable 'x'. As only h is assumed to be a stochastic variable, all other variables are not affected by the expectancy function.

Now, the problem therefore reduces to determining the expected values of E (h3) and E (h). As explained by Christensen [30], the probability density function, f(x), can be written in simple polynomial form as:

$$f(x) = \frac{35}{32c^7}\left(c^2 - x^2\right)^3 \qquad -c < x < c \qquad (19)$$
$$f(x) = 0 \qquad \text{elsewhere}$$

This polynomial function is the simplified approximated form of the Gaussian distribution. This simplification is important because the simplified expression of f(x) results in simpler formulation when expectancy operator is applied over

the functions of film thickness, 'h'. This function terminates at $\pm c$ where, $c = 3\sigma$ and σ is the standard deviation of the surface asperity height from the nominal value. The expected values of h and h^3 for the uniformly distributed asperities can be evaluated as:

$$E(h) = \int_{-\infty}^{+\infty} h \, f(x) \, dh = h \qquad (20)$$

$$E(h^3) = \int_{-\infty}^{+\infty} h^3 f(h) \, dh = h^3 + 3h\sigma^2 \qquad (21)$$

III. COMPUTATIONAL PROCEDURE

In the present study, FDM with non-uniform mesh discretization is adopted because of expected variation in the pressure gradients along the rolling direction. Fig. 3 shows computational domain discretization. As pressure gradients along the rolling direction in the contact region are very high, it requires a denser grid near the contact zone. Non-uniform meshing scheme along the direction of rolling is therefore considered more logical and appropriate for the solution of the present problem. The discretization in the outlet region and perpendicular to the rolling direction is performed with uniform meshing, because variation in the pressure gradient is relatively less in these directions. Non-uniform meshing is generated using the well-known geometrical progression. In the so called contact zone, Hertzian pressure is applied and outside the contact zone zero initial pressure is applied.
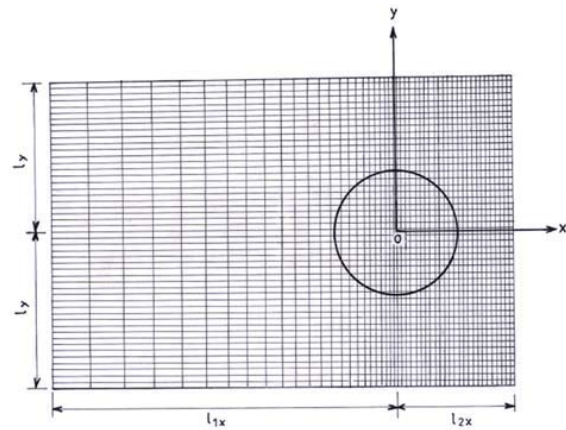

Fig. 3 Dizcritization of domain

$$p(i, j) = \frac{3FR}{2\pi ab\eta_0 u}\sqrt{1 - (x - m)^2 - (y - l)^2}$$
$$\text{if } (x - m)^2 + (y - l)^2 < 1.0$$

and outside the contact zone,

$$p(i, j) = 0.0 \quad \text{if } (x - m)^2 + (y - l)^2 \geq 1.0$$

Also, the pressure rises from zero reference value and then reduces to zero value smoothly without any discontinuity. To incorporate this feature in the solution, it must be ensured that $\frac{\partial p}{\partial x} = \frac{\partial p}{\partial y} = 0$ when $p = 0$. This is achieved simply by substituting $p = 0$ whenever $p < 0$. These boundary conditions are known as Reynolds boundary conditions. This approach is adopted since it is not known where $\frac{\partial p}{\partial x} = \frac{\partial p}{\partial y} = 0$ as it will be on the so called 'moving' boundary. Mathematically it is incorrect to say that if $p = 0$ then $\frac{\partial p}{\partial x} = \frac{\partial p}{\partial x} = 0$ but such a method works well here. The Reynolds equation is solved using the prescribed boundary conditions of input parameters. The pressure distribution obtained can then be integrated over the entire domain to provide the load carrying capacity. The traction coefficient can be estimated by the solution of traction model. The flow chart of the computation is shown in Fig. 4. The convergence criteria used for p (pressure) and T (temperature) are:

1. For p

$$|\left[\sum_j \sum_i p_{ij}\right]_{N-1} - \left[\sum_j \sum_i p_{ij}\right]_N | / |\left[\sum_j \sum_i p_{ij}\right]_N| \leq 10^{-6}$$
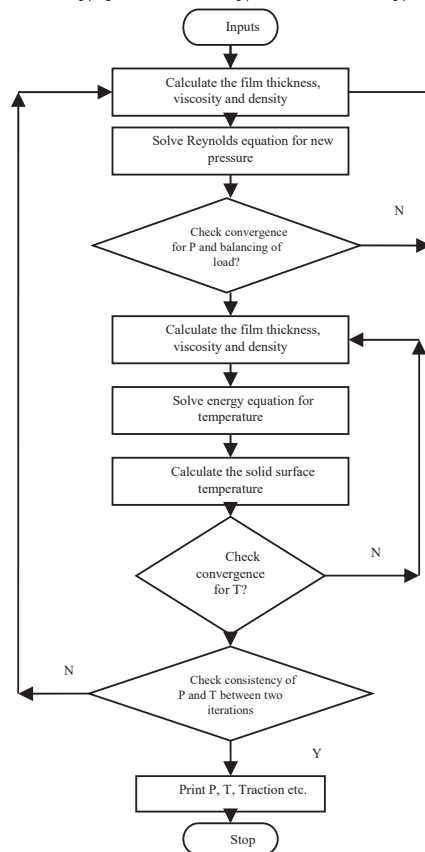
2. For T

$$|\left[\sum_j \sum_i T_{ij}\right]_{N-1} - \left[\sum_j \sum_i T_{ij}\right]_N | / |\left[\sum_j \sum_i T_{ij}\right]_N| \leq 10^{-2}$$

Fig. 4 Flow chart for computational procedure

IV. RESULTS AND DISCUSSION

In non-conformal contacts such as in rolling element bearings and gears etc., the estimation of minimum film thickness is an important requirement at the design stage. Moreover, in many applications, the ball bearings having EHL contacts are subjected to light loads, high rolling/sliding speeds, and starvation. Thus, awareness for the calculation of minimum film thickness as functions of load, rolling speed, material parameter, ellipticity ratio, roughness, slip, and starvation parameter, has vital importance for designers and maintenance engineers. In the elliptic EHL contacts, the increase of viscosity with pressure is one of the causes of the mating surfaces getting lubricated. However, high rolling/sliding speed generates huge heat in the lubricating film causing drastic reduction in lubricant viscosity. Therefore, for reliable operation of EHL contacts at high rolling/sliding speeds, it becomes important to determine the thermal effects on minimum film thickness prevailing between the mating surfaces. Due to the thinning of the lubricating oil at the concentrated EHL contacts having high rolling/sliding speeds and light loads, the escaping tendency of the lubricating oil increases. Thus, such contacts generally operate in starved conditions. Therefore, the thermal analyses of smooth and rough EHL elliptic contacts operating under lightly loaded and high rolling speeds, with fully flooded and starved conditions, have been carried out to achieve a correct estimate of the thermal effect on the minimum film thickness.
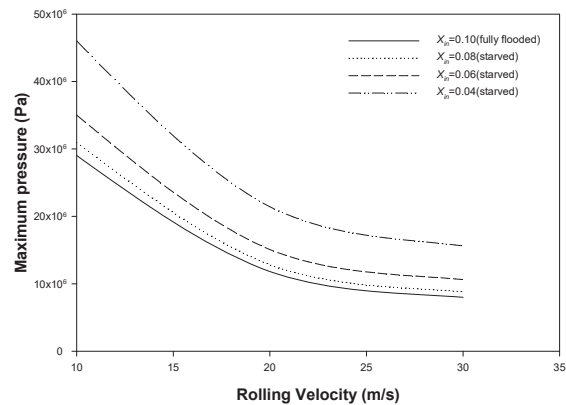

Fig. 5 Variation of maximum pressure with velocity at different starvation levels for load 8 N, ellipticity ratio 1, slip 0.5

Fig. 5 shows the variation of maximum pressure with velocity for different starvation levels. For a given speed the magnitude of maximum pressure rises sharply with the increase in level of starvation and the maximum pressure decreases with the increase in rolling velocity. This is due to the fact that at low rolling velocity the pumping action of the lubricant in the contact is less as compared to the high rolling velocity. Thus the effective domain under contact is less at lower rolling velocity and this causes relatively more pressure rise in the lubricant film at the low rolling velocity. However, the integration of pressure over the domain for any velocity results the same load carrying capacity.
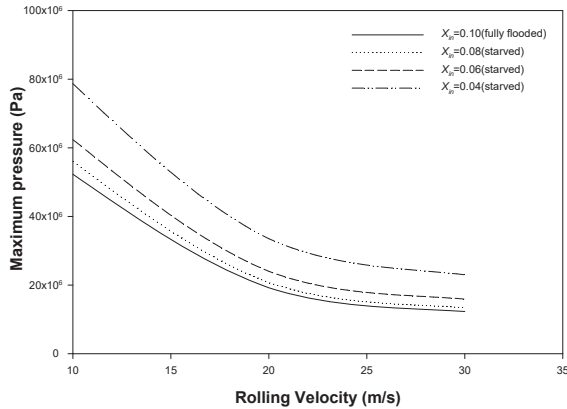
Fig. 6 Variation of maximum pressure with velocity at different
starvation levels for load 10 N, ellipticity ratio 1, slip 0.5

Fig. 6 shows the variation of maximum pressure with
rolling velocity at different starvation levels with the only
difference of the load being 10 N as compared to 8 N in Fig. 5.
For a given rolling speed, the magnitude of maximum pressure
rises sharply at 10 N in comparison to the values at 8 N. This
is due to the low film thickness at 10 N as compared to 8 N.
with the increase in ellipticity ratio the maximum value of the
pressure decreases marginally due to enhancement in the EHL
contact area for the given load. With increase in slip the
magnitude of maximum pressure reduces marginally with
other operating parameters remaining the same. This happens
due to the reduction in lubricant viscosity at higher slips. With
the increase in roughness there is marginal reduction in the
maximum pressure value which can be attributed to the
thinning of lubricant due to rise in velocity gradient. The
velocity gradient rises due to reduction of film thickness in the
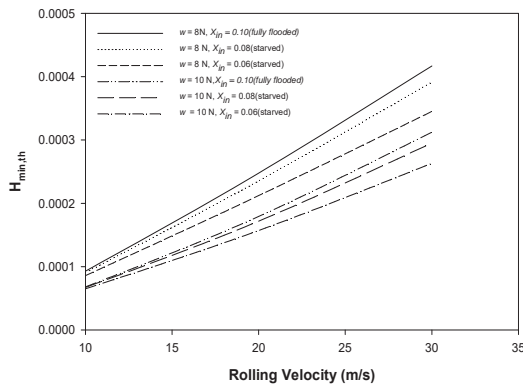presence of surface roughness.

Fig. 7 Variation of minimum thermal film thickness with velocity at
different starvation levels at various loads, ellipticity ratio 1, slip 0.5

Fig. 7 illustrates the influence of operating parameters on
the variation of minimum thermal film thickness along with
the change in rolling velocity and starvation levels. Minimum
thermal film thickness reduces considerably with the existence
of starvation in the EHL elliptic contacts. The trends of the
curve suggest that the effect of load on the minimum thermal

film thickness is significant at high rolling speeds. However,
the variation of minimum thermal film thickness with slip,
roughness and ellipticity ratio in EHL contacts are
comparatively small.

Using the computed results, regression analysis has been
performed to obtain the following dimensionless film
thickness formula

$$H_{th,min} = 0.879 W^{-1.2979} U^{1.2632} R_f^{-0.0249} X_{in}^{0.3897} S^{-0.0849} k^{0.0271}$$

where

$$8.66E\text{-}08 \leq W \leq 1.08E\text{-}07, \, 0.04 \leq X_{in} \leq 0.10,$$
$$8.9E\text{-}11 \leq U \leq 2.67E\text{-}10, \, 0.5 \leq S \leq 1,$$
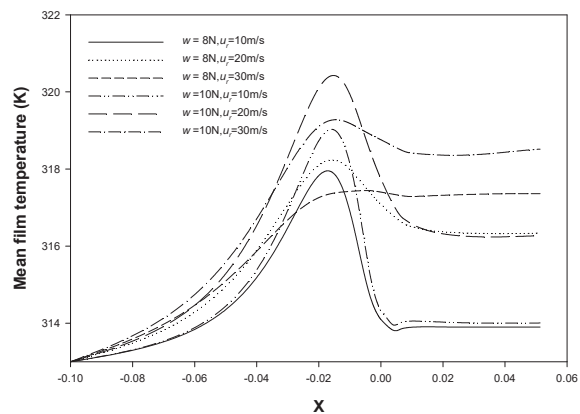$$1 \leq k \leq 5, \text{ and } 0 < R_f \leq 0.2$$

Fig. 8 Mean film temperature variation along the rolling direction
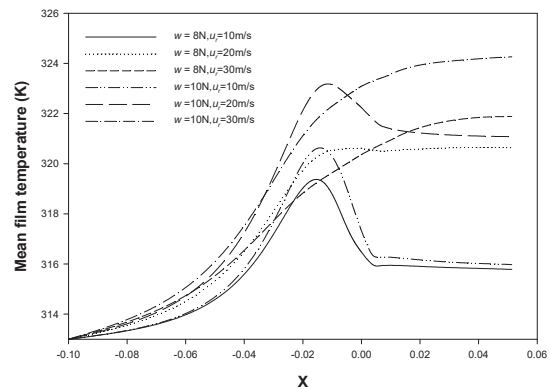with ellipticity ratio 5, slip 0.5

Fig. 9 Mean film temperature variation along the rolling direction
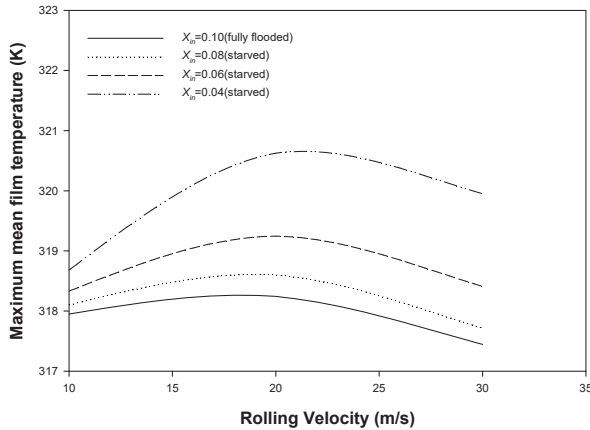with ellipticity ratio 5, slip 1.0

Fig. 10 Variation of maximum mean film temperature with Velocities at different starvation levels and load 8 N, ellipticity ratio 1, slip 0.5
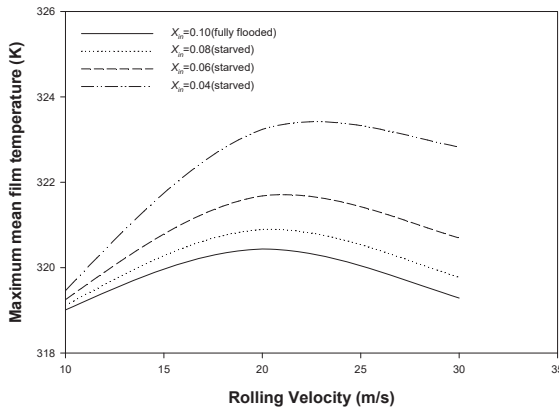

Fig. 11 Variation of maximum mean film temperature with Velocities at different starvation levels and load 10 N, ellipticity ratio 1, slip 0.5

In the failure of EHL non-conformal contacts, the thermal effect plays a detrimental role. It is well known by now that the thermal effects on the minimum film thickness and traction are significant in EHD lubricated contacts. An accurate estimation of maximum mean film temperature rise in the contact at various operating parameters is necessary for design and maintenance of contacts. Figs. 8 and 9 show the maximum mean film temperature distribution for slip 0.5 and 1.0 respectively, for loads of 8 N and 10 N and rolling velocity of 10 m/s, 20 m/s, 30m/s. The maximum mean film temperature at high load is more in comparison to low load at the same slip and rolling velocity. Trends of the temperature distribution demonstrate that for a given load, ellipticity ratio and slip maximum mean film temperature first rises with the increase in rolling velocity and at higher rolling velocity there is decline in maximum mean film temperature. This is due to the effect of convection cooling, which is predominant at high rolling velocities. It is seen that due to increase in ellipticity ratio and roughness there is negligible change in maximum mean film temperature. Variation of maximum mean film temperature with rolling velocity at different starvation levels is shown in Figs. 10 and 11. These figures demonstrate that

with the increase in starvation level, the maximum mean film temperature rise is substantial.

Using the computed results, regression analysis has been performed to obtain the following maximum mean film temperature rise formula

$$\Delta t = 3.9489 \times 10^8 W^{1.1316} U^{0.2591} R_f^{-0.0069} X_{in}^{-0.2898} S^{0.5566} k^{0.004}$$

where

$$8.66\text{E-}08 \leq W \leq 1.08\text{E-}07, \; 0.04 \leq X_{in} \leq 0.10,$$
$$8.9\text{E-}11 \leq U \leq 2.67\text{E-}10, \; 0.5 \leq S \leq 1,$$
$$1 \leq k \leq 5, \text{ and } 0 < R_f \leq 0.2$$
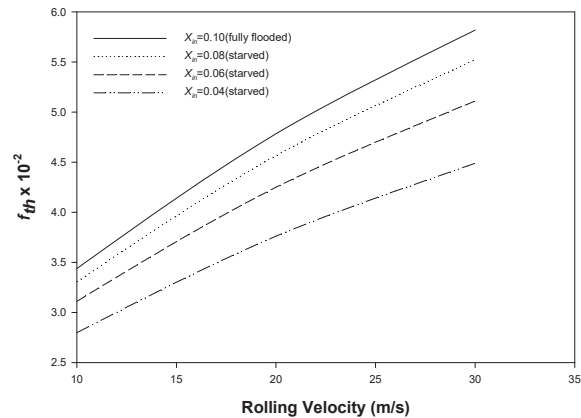
Fig. 12 Variation of traction with velocity for different starvation levels, load 8 N, ellipticity ratio 1, slip 1.0
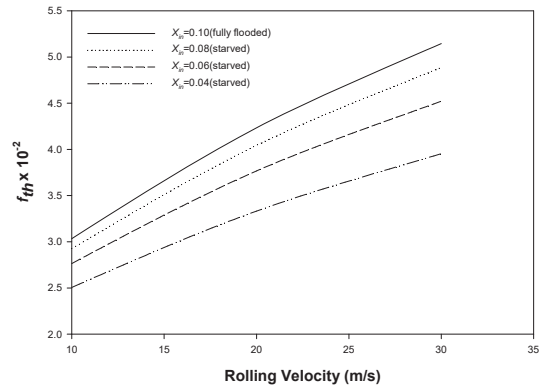
Fig. 13 Variation of traction with velocity for different starvation levels, load 10 N, ellipticity ratio 1, slip 1.0

An accurate estimate of traction coefficient due to rolling/sliding is essential from view point of power loss calculation and to study the failure of lubrication in starved contacts. The traction coefficient for lubricating film under EHL elliptic contacts has been computed herein for the provided in Table I.

TABLE I
MATERIAL PROPERTIES

Elastic modulus (E_1, E_2), GPa	2.06
Thermal conductivity (k_s), W/m-K	46
Density (ρ_0), kg/m³	7850
Specific heat (C_{ps}), J/kg-K	470
Equivalent radius (R), m	0.02
Poisson's ratio (v_1, v_2)	0.3
Inlet viscosity (η_0), Pa-s	0.0411
Pressure viscosity coefficient (α), m²/N	1.591 x 10⁻⁸
Inlet density (ρ_0), kg/m³	846
Specific heat (C_p), J/kg-K	2000
Inlet temperature of the lubricant (T_0), K	313
Thermal expansivity coefficient (β)	6.4 x 10⁻⁴
Temperature viscosity coefficient (γ), K⁻¹	0.042
Thermal conductivity (k_f), W/m-K	0.14

Major mechanism of heat generation in the contact is viscous shear heating while the mechanism of heat removal is conduction across the film and convection along the film. Figs. 12 and 13 show the variation of traction coefficient for fully flooded and starved EHL contacts operating under various conditions. It is seen that thermal effects on traction coefficients are significant at high rolling velocities. With the increase in the level of starvation the traction reduces considerably due to shearing of less quantity of lubricating oil present in the contact due to starvation effects. Roughness and ellipticity ratio are found to have very little effect on traction coefficient. Load, Slip and rolling velocity have a significant effect on the traction coefficient as can be seen from the figures. Using the computed results, regression analysis has been performed to obtain the following dimensionless film thickness formula

$$ f_{th} = 0.4753 W^{-0.5047} U^{0.4477} R_f^{0.016} X_{in}^{0.2112} S^{0.6386} k^{-0.0069} $$

where

$$ 8.66\text{E-}08 \leq W \leq 1.08\text{E-}07, \, 0.04 \leq X_{in} \leq 0.10, $$

$$ 8.9\text{E-}11 \leq U \leq 2.67\text{E-}10, \, 0.5 \leq S \leq 1, $$

$$ 1 \leq k \leq 5, \text{ and } 0 < R_f \leq 0.2 $$

V. CONCLUSION

An efficient and accurate analysis of EHL elliptic contact has been achieved. The importance of this work lies in the fact that it presents for the first time empirical relations of minimum film thickness and maximum mean film temperature rise for EHL elliptic contacts operating under fully flooded and starved conditions at light loads, high rolling speeds, and high slips. These relations are expected to be very useful in design of EHL contacts of rolling element bearings and gears. The analysis used is general and can also be extended to EHL elliptic contact analysis for non-Newtonian lubricant rheology.

NOMENCLATURE

a:	length of semi minor axis (m) = $\left\{ (3wR_x)/(2E') \right\}^{1/3}$
b:	length of semi major axis (m) = ka
c:	asperity height (m)
c_1, c_2:	specific heat of solids 1 and 2, respectively (J/kg-K)
C_p:	specific heat of lubricant (J/kg-K)
$d(0,0)$:	deformation in z-direction at origin (m)
$d(i,j)$:	elastic deformation in z-direction at a general node (m)
$E(x)$:	expectancy function = $\int_{-\infty}^{+\infty} x\, f(x)dx$
E_1, E_2:	modulus of elasticity of solids 1 and 2, respectively (N/m²)
E':	equivalent modulus of elasticity = $2.0/\left(\frac{1-v_1^2}{E_1} + \frac{1-v_2^2}{E_2} \right)$ N/m²
$f(x)$:	probability density function
f_{th}:	traction coefficient
F:	tractive force (N)
$h(x)$:	film thickness (m)
$h(x,y,z)$:	lubricant film thickness characterized in 3-D domain (m)
h_c:	central film thickness (m)
h_0:	minimum film thickness with rigid ball (m)
$h_n(x,y,z)$:	normal or smooth film thickness (m)
$h_s(x,y, \xi$):	film thickness component due to roughness (m)
$H_{min.,th}$:	dimensionless thermal minimum film thickness (m)
k:	ellipticity ratio
k_f:	thermal conductivity of lubricant (W/m-K)
k_1, k_2:	thermal conductivities of solids 1 and 2, (W/m-K)
l:	length of half computational domain in y direction (m)
m:	length of inlet zone (m)
m_1, m_2:	lengths related to pressure element (m)
n:	length of outlet zone (m)
n_1, n_2:	lengths related to pressure element (m)
η:	viscosity of lubricant (Pa-s)
η_0:	viscosity of lubricant at T_0 (Pa-s)
p:	pressure (N/m²)
P_H:	Hertzian pressure (N/m²)
R_x, R_y:	equivalent radii of solids in x-z and y-z planes, (m)
R_f:	roughness factor (expressed as percentage of $H_{min,iso}$
S:	slide to roll ratio, $(u_1 - u_2)/u_r$
Δt :	dimensionless maximum mean film temperature rise, $(T_m - T_0)/T_0$
T:	temperature (K)
$T(x,y,z)$:	temperature in the film domain at a general location (K)
T_1, T_2:	temperatures of the bounding surfaces 1 and 2, (K)
T_m:	mean film temperature (K)
T_0:	inlet temperature (K)
u:	velocity in x direction (m/s)
u_1, u_2:	rolling velocities of solids 1 and 2, respectively (m/s)
u_r:	rolling velocity, $(u_1 + u_2)/2$ (m/s)
U:	dimensionless rolling velocity, $(u_r \times \eta_0)/(E' \times R_x)$
w:	load (N)
W:	dimensionless load, $w/(E' \times R_x^2)$
x,y,z:	coordinates in three directions (m)
z' :	Reoland's viscosity exponent
X:	dimensionless coordinate in x-direction
Y:	dimensionless coordinate in Y-direction
X_{in}:	dimensionless length for inlet zone
x', y' :	local coordinates (m)
β :	thermal expansivity coefficient (K⁻¹)

γ :   temperature viscosity coefficient (K^{-1})

ρ_0 :   density of lubricant at T_0 (kg/m^3)

σ :   standard deviation of the surface asperity height

ψ :   dummy variable

$\tau_{0,h}$:   shear stresses at surfaces 1 and 2, respectively (N/m^2)

ξ :   random variable

REFERENCES

[1] Archard, J. F. and Kirk, M. T., "Lubrication at Point Contacts", Vol. 261, Proc. Roy Soc, London, Series A, 1961, pp. 532 - 550.

[2] Crook, A. W., "Elastohydrodynamic Lubrication of Rollers", Vol. 190, Nature, 1961, pp. 1182 - 1183.

[3] Kapitza, P. L., "Hydrodynamic Theory of Lubrication during Rolling", Vol. 25(4), Zh. Tekh. Fiz, 1955, pp. 747 - 762.

[4] Cameron, A. and Gohar, R., "Theoretical and Experimental Studies of the Oil Film in Lubricated Point Contact", Vol. 291, Proc. Roy Soc, London, Series A, 1966, pp.520 - 536.

[5] Archard, J. F., Cowking, E. W., "Elastohydrodynamic Lubrication at Point Contacts", Vol. 180, Proc. Instn Mech Engrs, London, 1966, pp. 47 -56.

[6] Cheng, H. S., "A Numerical Solution to the Elastohydrodynamic Film Thickness in an Elliptical Contact", Vol. 92, ASME Trans, Journal of Lubrication Technology, 1970, pp. 155 - 162.

[7] Ranger, A. P., Ettles, C. M. M., Cameron, A., "The Solution of the Point Contact Elastohydrodynamic Problem," Vol. 346, Proc Roy Soc, London, Series A, 1975, pp. 227 - 244.

[8] Dowson, D., Hamrock, B. J., "Numerical Evaluation of the Surface Deformation of Elastic Solids Subjected to a Hertzian Contact Stress" Vol. 19 (4), ASLE Trans, 1976, pp. 279 - 286.

[9] Biswas, S., Snidle, R. W., "Calculation of Surface Deformation in Point Contact EHD" Vol. 99, ASME Trans, Journal of Lubrication Technology, 1977, pp. 313 - 317.

[10] Hamrock, B.J., Dowson, D., "Isothermal Elastohydrodynamic lubrication of Point Contacts, Part II- Ellpticity Parameter Results" Vol. 98 (3), ASME Trans, Journal of Lubrication Technology, 1976, pp. 375 - 383.

[11] Hamrock, B.J., Dowson, D., "Isothermal Elastohydrodynamic lubrication of Point Contacts, Part III- Fully flooded Results" Vol. 99(2), ASME Trans, Journal of Lubrication Technology, 1977, pp. 264-276.

[12] Hamrock, B.J., Dowson, D., "Isothermal Elastohydrodynamic lubrication of Point Contacts, Part IV- Starvation Results" Vol. 99 (1), ASME Trans, Journal of Lubrication Technology, 1977, pp. 15-23.

[13] Evans, H.P., Snidle, R.W., "Inverse Solution of Reynolds' Equation of Lubrication under point Contact Elastohydrodynamic conditions" Vol. 103, ASME Trans, Journal of Lubrication Technology, 1981, pp. 539-546.

[14] Venner, C.H., Napel, W.E., "Multilevel Solution of the Elastohydrodynamically Lubricated Circular Contact Problem Part 1: Theory and Numerical Algorithm" Vol.152, Wear, 1992, pp. 351-367.

[15] Venner, C.H., Napel, W.E., "Multilevel Solution of the Elastohydrodynamically Lubricated Circular Contact Problem Part 2: Smooth Surface Results" Vol.152, Wear, 1992, pp. 369-381.

[16] Brewe, D.E., Hamrock, B.J., "Analysis of starvation effects on hydrodynamic lubrication in nonconforming contacts," Vol. 104, ASME Trans, Journal of Lubrication Technology, 1982, pp. 410-417.

[17] Gentle, C.R., Pasdari, M., "Computer simulation of starvation in thrust loaded ball bearings," Vol. 92, Wear, 1983, pp. 125-134.

[18] Bruggemann, H., Kollmann, F.G., "A Numerical Solution to the Thermal Elastohydrodynamic Lubrication in an Elliptical contact" Vol. 104, ASME Trans, Journal of Lubrication Technology, 1982, pp. 392-400.

[19] Kim, K.H., Sadeghi, F., "Three dimensional Temperature distribution in EHD Lubrication: Part I- circular Contact" Vol. 114, ASME Trans, Journal of Tribology, 1992, pp. 32-41.

[20] Kim, K.H., Sadeghi, F., "Three dimensional Temperature distribution in EHD Lubrication: Part II- Point Contact and Numerical formulation" Vol. 115, ASME Trans, Journal of Tribology, 1993, pp. 36-45.

[21] Salehizadeh, H., Saka, N., "Thermal Non- Newtonian Elastohydrodynamic Lubrication of Rolling Line Contact" Vol. 113, ASME Trans, Journal of Tribology, 1991, pp. 481-491.

[22] Wolf, R., Kubo, A., "The Application of Newton – Raphson Method to Thermal Elastohydrodynamic Lubrication of Line Contacts" Vol. 116, ASME Trans, Journal of Tribology, 1994, pp. 733-740.

[23] Kazama, T., Ehret, P., Taylor, C.M., "On the effects of the Temperature Profile Approximation in the Thermal Newtonian Solutions of Elastohydrodynamic Line Contacts" Vol. 215, Proc. Instn Mech Engrs, London, Journal of engineering Tribology, Part J, 2001, pp. 109-120.

[24] Jiang, X., Wong, P.L., Zhang, J., "Thermal Non –Newtonian EHL Analysis of Rib – Roller End Contact in Tapered Roller Bearings" Vol. 117, ASME Trans, Journal of Tribology, 1995, pp. 646-654.

[25] Lee, R.T., Hsu, C.H., Kuo, W.F., "Multilevel Solution for Themal Elastohydrodynamic Lubrication of Rolling/Sliding Circular Contacts, Vol. 28 (J8), Tribology International, 1995, pp.541-552.

[26] Ehret, P., Dowson, D., Taylor, C.M., "Thermal Effects in the Elliptic Contacts with Spin Conditions" Proceedings of the 25th Leeds - Lyon Conference on Tribology, Tribology for Energy Conservation 36, 1999, pp.685-703.

[27] Gang, X., Sadeghi, F., "Thermal EHL Analysis of Circular Contact with Measured Surface Roughness" Vol. 118, ASME Trans, Journal of Tribology, 1996, pp. 473-483.

[28] Zhu, D., Hu, Y. Z., "A Computer Program Package for the Prediction of EHL and Mixed Lubrication Characteristics, Friction, Subsurface Stresses and flash Temperatures Based on Measured 3-D Surface Roughness" Vol. 44, Tribology Transactions,2001, pp.42-49.

[29] Yang, P., Qu, S., Kaneta, M., Nishikawa, H., "Formation of Steady Dimples in Point TEHL Contacts," Vol. 123, ASME Trans, Journal of Tribology, 2001, pp. 42-49.

[30] Christensen, H., "Stochastic models for Hydrodynamic Lubrication of Rough Surfaces," Vol. 184, Proc. Instn Mech Engrs, London, 1970, pp. 1013-1026.